Biological Trace Element Research
https://doi.org/10.1007/s12011-024-04167-8

RESEARCH

LINC00942 Alleviates $NaAsO_2$-induced Apoptosis by Promoting GSH Synthesis Through Targeting miR-214-5p

Mingxiao Ma[1,2] · Jingyi Zhang[1,2] · Sheng Li[1,2] · Mengyao Zhang[1,2] · Weixin Chen[1,2] · Linzhi Li[1,2] · Shugang Li[3]

Received: 22 January 2024 / Accepted: 28 March 2024

Abstract

The mechanism of arsenic-induced liver toxicity is not fully understood. This study aimed to investigate the role of LINC00942 in arsenic-induced hepatotoxicity by regulating miR-214-5p. As the exposure dose of $NaAsO_2$ gradually increases, cell viability, intracellular GSH content, ΔΨm, and the protein levels of GCLC and GCLM were reduced significantly. Apoptosis rate, ROS, and expression of apoptosis-related and NF-κB pathway proteins increased. The expression of LINC00942 was increased, while the expression of miR-214-5p was decreased. After suppressing LINC00942 levels, $NaAsO_2$ exposure further decreased cell viability, intracellular GSH content, ΔΨm, GCLC protein, and miR-214-5p expression. The apoptosis rate, ROS, and apoptosis-related and NF-κB pathway proteins further increased. miR-214-5p is targeted and negatively regulated by LINC00942. After miR-214-5p was overexpressed, $NaAsO_2$ further decreased cell viability, intracellular GSH content, ΔΨm, and GCLC protein expression compared to $NaAsO_2$ exposure. The apoptosis rate, ROS, apoptosis-related and NF-κB pathway proteins p65, and IKKβ were higher than those exposed to $NaAsO_2$. LINC00942 inhibitor along with miR-214-5p inhibitor combined with $NaAsO_2$ treatment resulted in increased cell viability, GSH, Bcl-2, and GCLC protein expression and decreased apoptosis rate, apoptosis related, p65, IKKβ protein, and ΔΨm, as compared to the combined $NaAsO_2$ and si LINC00942 group. $NaAsO_2$ exposure induces oxidative damage and apoptosis in LX-2 cells by activating NF-κB and inhibiting GSH synthesis. During this process, the expression level of LINC00942 increases, targeting to reduce the level of miR-214-5p, then weakening the effect of $NaAsO_2$ on NF-κB, thereby alleviating cellular oxidative damage and playing a protective role.

Keywords Arsenic · LINC00942 · miR-214-5p · NF-κB · Apoptosis · Oxidative damage

Introduction

Arsenic and its compounds exist widely in nature and can be absorbed by humans in different ways. Exposure to arsenic compounds continues to pose substantial public health concerns for hundreds of millions of people around the globe [1]. The liver is an important target organ for arsenic toxicity. Oxidative stress-induced lipid peroxidation is considered to be one of the important mechanisms of arsenic hepatotoxicity. Glutathione (GSH) is a substance that maintains redox homeostasis in cells, which regulates hepatocyte apoptosis caused by oxidative damage [2]. The pathway that NF-κB downregulates the level of GCLC to inhibit GSH synthesis plays a crucial role in arsenic-induced apoptosis [3]. However, the specific mechanism has not yet been fully elucidated.

MicroRNAs (miRNAs) are small non-coding RNA molecules that regulate gene expression by binding to the 3' untranslated region (3'-UTR) of target genes, inhibiting mRNA translation or stimulating mRNA degradation. It plays a role in the inflammation, proliferation, and apoptosis of liver cells [4–6]. MiR-214 is a product of the 110 bp miR-214 gene in the intron of the Dynamin-3 gene on human

Mingxiao Ma and Jingyi Zhang contributed equally to this work.

✉ Shugang Li
lishugang@ccmu.edu.cn

[1] Department of Preventive Medicine, School of Medicine, Shihezi University, Shihezi, Xinjiang, China

[2] Key Laboratory for Prevention and Control of Emerging Infectious Diseases and Public Health Security, the Xinjiang Production and Construction Corps, Shihezi, China

[3] Department of Maternal and Children Health, School of Public Health, Capital Medical University, Beijing 100069, China

Published online: 05 April 2024

chromosome 1-NC_000001.10. MiR-214-5p is processed from the 5' arm of the miR-214 precursor and is involved in coordinating a variety of physiological processes, which plays a role in in liver detoxification [7]. In addition, miR-214-5p also regulates the process of arsenic-induced oxidative stress [8]. Recent studies have found that miR-214-5p can not only regulate the level of intracellular GSH to participate in oxidative stress [9] but also promote the activation of the NF-κB signaling pathway to induce apoptosis [10]. Many studies have found that miRNAs are regulated by long non-coding RNAs (LncRNA) and participate in the process of cell oxidative damage and apoptosis [11–13]. lncRNA RMRP regulates the expression of p53 and induces apoptosis of H9C2 cells by targeting miR-214-5p [14]. At the same time, on the website (http://mircode.org/), it was predicted that miR-214-5p may have a potential target binding site with LINC00942.

Long non-coding RNA is a non-coding RNA with a transcription length of more than 200 nt, which plays a role in cell differentiation, proliferation, and apoptosis [15]. LncRNAs can regulate cellular oxidative damage by affecting the NF-κB signaling pathway through binding to the 3'-untranslated region of miRNAs; e.g., LncRNA NEAT1 can promote oxidative damage in renal tubular epithelial cells by activating the TLR4/NF-κB pathway through targeted inhibition of miR-130a-3p [16]. Long intergenic non-protein coding RNA 00942 (LINC00942) is located on chromosome 21 and can be involved in the regulation of cell proliferation by targeting METTL14 protein [17], PI3K/mTOR [18], etc. It has been reported that LINC00942 is also involved in the transcription process of GCLC [19], but the role of LINC00942 in hepatocyte apoptosis by arsenic-induced oxidative damage has rarely been reported.

In summary, arsenic can inhibit the synthesis of GSH and induce apoptosis by activating the NF-κB pathway, and the regulation of miR-214-5p by arsenic can also regulate the expression of related proteins in the NF-κB pathway. LINC00942 may target miR-214-5p and affect the expression of GCLC, a key enzyme subunit of GSH synthesis. However, it has not been reported whether arsenic can affect NF-κB by regulating miR-214-5p through LINC00942. In the present study, the human liver LX-2 cell was treated with different concentrations of $NaAsO_2$ and si LINC00942, miR-214-5p mimic to illuminate the function and mechanism of LINC00942, miR-214-5p in arsenic-induced apoptosis.

Materials and Methods

Cell Culture and Treatments

LX-2 cell line was purchased from Wuhan Procell Life Technology Co., Ltd. (CL-0560, Wuhan). It is an immortalized cell line obtained from human liver stellate cells transfected with SV40 T antigen, which retains the key characteristics of liver stellate cells such as signal transduction gene expression. The cells were cultured in DMEM medium (Grand Island, NY, USA) supplemented with 10% fetal bovine serum (South America) and 1% penicillin–streptomycin (Beyotime, Shanghai, China) in an atmosphere of 5% CO_2 at 37 °C. Based on our previous research [3], LX-2 cells were exposed to $NaAsO_2$ at concentrations of 0 μM, 10 μM, 15 μM, 20 μM, and 25 μM for 24 h or 15 μM for 12 h, 24 h, and 48 h.

Wright's Giemsa Staining

LX-2 cells were cultured in 6-well plates according to the preset grouping, then operated according to the instructions of the modified Giemsa staining solution, and observed with an optical microscope.

Cell Viability Detection

Cell Counting Kit-8 (Beyotime, Shanghai, China) was used to determine cell viability. The cells were cultured in 96-well plates with a volume of 100 μL/well (1×10^4 cells/well). After treatment, 10 μL CCK8 solution was added to each well, incubated at 37 ℃ and 5% CO_2 for 3 h, and the absorbance was measured at 450 nm with a microplate reader. Finally, cell viability is calculated according to the following formula. In the formula, the OD value is optical density, the control group is the untreated LX-2 cell group, the experimental group is the treated LX-2 cell group, and the blank group is the solvent control group.

$$Cell\ Vibility = \frac{(\text{OD value of the experimental group} - \text{OD value of blank group})}{(\text{OD value of control group} - \text{OD value of blank group})} \times 100\%$$

Apoptosis Rate

Treated LX-2 cells were collected, washed twice with 4 ℃ PBS, and mixed in 50 μl sample buffer. Then, 5 μl Annexin V-FITC and 2.5 μl propidium iodide were added to the mixed cells for staining. After 10 min of incubation without light, the apoptotic cells were detected using flow cytometry.

Cellular Mitochondrial Membrane Potential

Cells were digested with trypsin and washed twice with PBS; 1 ml of JC-1 staining solution was added to each well, mixed, and incubated at 37 °C, 5% CO_2 for 20 min. Cells were centrifuged at 600 g, 4 ℃ for 4 min, washed twice with JC-1 staining buffer, resuspended, and analyzed by flow cytometry.

GSH Content Detection

The GSH content in the cells was detected by trace reduced glutathione (GSH) assay kit (Beyotime, Shanghai, China) after collecting processed cells, operating according to the instruction of the kit, using a microplate reader to detect the absorbance at 405 nm, and then calculating the concentration of GSH in the cells according to the formula.

Active Oxygen Detection

The intracellular ROS levels were detected using a 2',7'-dichlorofluorescein diacetate (DCFH-DA) fluorescent probe. After collecting the cells, 1 mL of 10 μM DCFH-DA was added to each tube, incubated for 20 min at 37 °C in a 5% CO_2 incubator, washed twice with serum-free DMEM, resuspended, and analyzed by flow cytometry.

Mitochondrial Morphology

Cells were digested with trypsin for 1 min and centrifuged at 1000 rpm/min for 2 min, and the cell pellets were deposited at the bottom of the EP tube; normal temperature fixative solution containing 2.5% glutaraldehyde was added. After fixing it at room temperature in the dark, transfer it to a 4 °C refrigerator for storage in the dark. After mixing acetone and isoamyl acetate at a ratio of 1:1, the fixed sample was dehydrated for 10 min, followed by dehydration in isoamyl acetate reagent for 30 min, then soaked in 50% acetonitrile solution, 70% acetonitrile solution for 15 min, and acetonitrile solution with increasing concentration of 10% for the same time, and finally vacuum dried after soaking in 95% and 100% acetonitrile solution. When the sample was dried and returned to room temperature, the air was released, and the sample was observed with a transmission electron microscope.

Plasmid Transfection

Si LINC00942, si NC, miR-214-5p inhibitor, inhibitor NC, miR-214-5p mimic, and mimic NC (Gemma, Shanghai) were transiently transfected into LX-2 cells using Lipofectamine 2000 (Invitrogen, USA) according to plasmid transfection instructions. After 5 h of transfection, the subsequent intervention experiments were continued after removing the transfection medium.

qRT-PCR

RT-PCR was performed to detect the expression levels of LINC00942 and miR-214-5p. Total RNA was extracted using Trizol® Reagent, and 5 μl of total RNA was used as a template for cDNA synthesis at a final concentration of 200 ng/μl according to the instructions of the ReverTrAce PCR RT kit. Reverse transcription was performed in the presence of 5 × RT buffer, RT enzyme mix, and primer mix. SYBR Green Realtime PCR Master Mix-Plus kit was used with 1 ng cDNA as a template, GAPDH as an internal reference, and U6 as an internal reference for miR-214-5p. The Quant Studio 6 Flex system was used for real-time fluorescence quantification. For primer sequences, see Table 1.

Western Blot

Cells were lysed with cell lysis buffer (RIPA: PMSF: phosphatase inhibitor, 100:1:1). Protein concentration was detected using the BCA protein concentration assay kit (Beyotime Biotechnology, P0010, CHINA). Proteins were separated by SDS-PAGE gel electrophoresis and transferred to PVDF membranes under 300 mA constant current. The PVDF membrane was then blocked with 0.1% Tween 20 and 5% skimmed milk powder or 5% BSA for 1.5 h. PVDF membranes were incubated with anti-NF-κBp65 antibody (ab16502, abcam), anti-IKK-β antibody (#8943, Cell Signaling Technology), anti-GCLM antibody (ab126704, abcam), anti-GCLC antibody (ab207777, abcam), anti-Caspase 3 antibody (19,677–1-AP, proteintech), anti-Bcl-2 antibody (12,789–1-AP, proteintech), anti-BAX antibody (50,599–2-Ig, proteintech), anti-Cleaved-Caspase 3 antibody (ab32042, abcam), and anti-GAPDH monoclonal antibody (TA-08, ZSGB-BIO) primary antibodies, which

Table 1 PCR primer sequence

Gene	Primer	Sequence (5'-3')
GAPDH	Forward	GGAAGCTTGTCATCAATGGAAATC
	Reverse	TGATGACCCTTTTGGCTCCC
U6	Forward	CTCGCTTCGGCAGCACA
	Reverse	AACGCTTCACGAATTTGCGT
HmiR-214-5p	Forward	TGGTGTCGTGGAGTCG
	Reverse	ACACTCCAGCTGGGTGCCTGTCTA CACTTG
LINC00942	Forward	AAATTATCAGCACAGCTTGGG
	Reverse	CACAGACCTTCCTCGGTTG

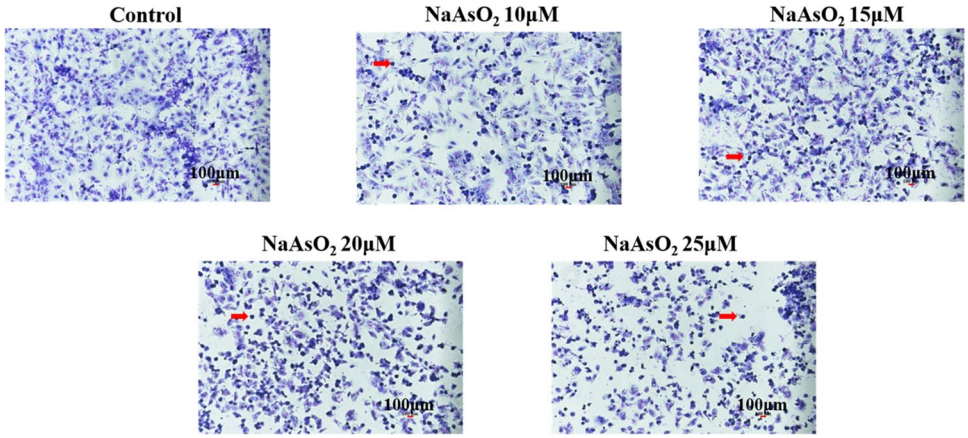

Fig. 1 Effect of different concentrations of $NaAsO_2$ on cell morphology. The red arrow in the figure points to the apoptotic deep-stained cell, the magnification is × 40, and the scale bar is 100 μm

were incubated overnight at 4 °C. In a membrane reaction coupled to horseradish peroxidase and horseradish enzyme-labeled goat anti-rabbit IgG (H + L) (ZB-2301, ZSGB-BIO) or biotinylated goat anti-mouse IgM (ZB-2055, ZSGB-BIO). Reactions were detected by chemiluminescence. The intensity of the bands was quantified using Image J software.

FluorescenceIn SituHybridization

The localization of LINC00942 and miR-214-5p in LX-2 cells was determined by FISH. Cells were fixed

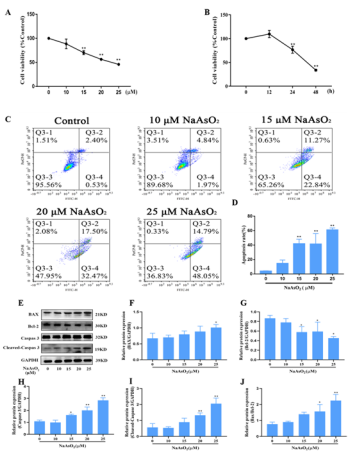

Fig. 2 Effect of different concentrations of $NaAsO_2$ on cell viability and apoptosis. **A** The viability of LX-2 cells after exposure to different concentrations of $NaAsO_2$ for 24 h. **B** The viability of LX-2 cells after exposure to 15 μM $NaAsO_2$ at different times. **C** The level of apoptosis of LX-2 cells detected by flow cytometry Q3-1, Q3-2, Q3-3, and Q3-4 indicates mechanically injured cells, late apoptotic cells, normal cells, and early apoptotic cells. **D** Quantitative data on apoptosis rates of cells treated with different concentrations of $NaAsO_2$. **E**, **F** Western blotting images and quantitative data of relative expression level of BAX, Bcl-2, caspase 3, cleaved-caspase 3, and Bax/Bcl-2. *It indicates a comparison with the control group, $P < 0.05$. **It indicates a comparison with the control group, $P < 0.01$, $n = 3$

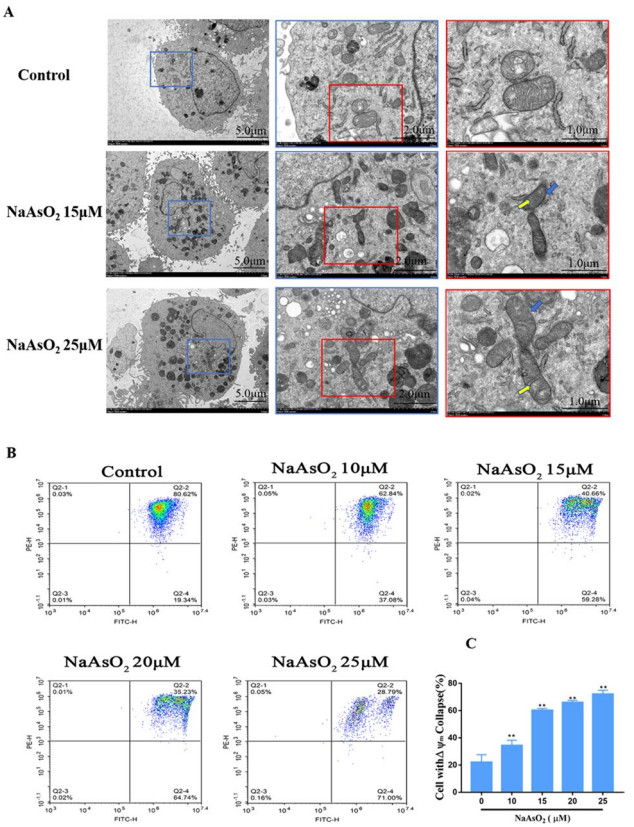

Fig. 3 Effects of different concentrations of $NaAsO_2$ on mitochondria of LX-2 cells. **A** Cellular mitochondrial structures were observed using transmission electron microscopy. The first column represents the structures of different groups of LX-2 cells and mitochondria at × 2.0 k Zoom, with a scale bar of 5.0 μm; the second column represents the cellular and mitochondrial structures of the blue part of the first column observed at × 7.0 k Zoom, with a scale bar of 2.0 μm; the third column represents the cellular and mitochondrial structures of the red part of the second column observed at 15.0 k Zoom, scale bar is 1 μm. Blue arrowheads indicate the outer mitochondrial membrane, and yellow arrowheads indicate the mitochondrial cristae. **B** Effect of different concentrations of $NaAsO_2$ on mitochondrial membrane potential. **C** Quantitative data on mitochondrial membrane potential treated with different concentrations of $NaAsO_2$. **It indicates a comparison with the control group, $P < 0.01$, $n = 3$

with 4% paraformaldehyde and operated according to the instructions, and fluorescently labeled probes were used for hybridization, respectively. The nuclei of LX-2 cells were stained using DAPI (Beyotime, Shanghai, China).

Dual Luciferase Reporter Assay

Plasmids were constructed with miR-214-5p mutated to the wild-type LINC00942-3'-UTR (WT) binding site. Sea kidney luciferase and firefly luciferase sequences were constructed into reporter fluorescent plasmid vector and internal reference plasmid vector, respectively. The constructed reporter plasmids were co-transfected with cells. Then the luciferase activity was detected using a dual luciferase reporter system to determine the targeting site of action of LINC00942 and miR-214-5p.

Statistical Methods

Statistical analyses were performed using GraphPad Prism 8.0 software. Mean ± SD was used to express the expression of cell viability, apoptosis, redox-related index genes, and proteins. Comparisons between multiple groups were performed using one-way ANOVA. Tukey's multiple test was used for multiple comparisons among groups. Statistical significance was set at $P < 0.05$.

Results

The Effect of $NaAsO_2$on the Morphology, Cell Viability, and Apoptosis of LX-2 Cells

Morphological changes of cells treated with $NaAsO_2$ using Wright's Giemsa staining. The typical morphological features of cell apoptosis, including cell shrinkage and loss of normal nuclear architecture, were observed in the $NaAsO_2$-treated group under the light microscope, which was not observed in the control group (Fig. 1).

To analyze the effect of $NaAsO_2$ exposure, we exposed LX-2 cells to different concentrations of $NaAsO_2$ (10 μM, 15 μM, 20 μM, and 25 μM) and measured cell viability and apoptosis rate. Cell viability was significantly decreased (Fig. 2A), and apoptosis rate was significantly increased at 15 μM (Fig. 2C,D). Then, we treated the cells with 15 μM $NaAsO_2$ at different times (12 h, 24 h, and 48 h). The cell viability decreases significantly when the time reaches 24 h (Fig. 2B). The expression levels of apoptotic proteins caspase 3, cleaved-caspase 3, and BAX/Bcl-2 were increased after $NaAsO_2$ treatment (Fig. 2E–J) (all $P < 0.05$).

$NaAsO_2$ Induces Oxidative Stress by Activating NF-κB and Inhibiting GCLC Signaling Pathway

It was found that the nuclear membrane of the control cells was intact. The mitochondrial membrane was clear and connected to the ridge, which became tubular. There were

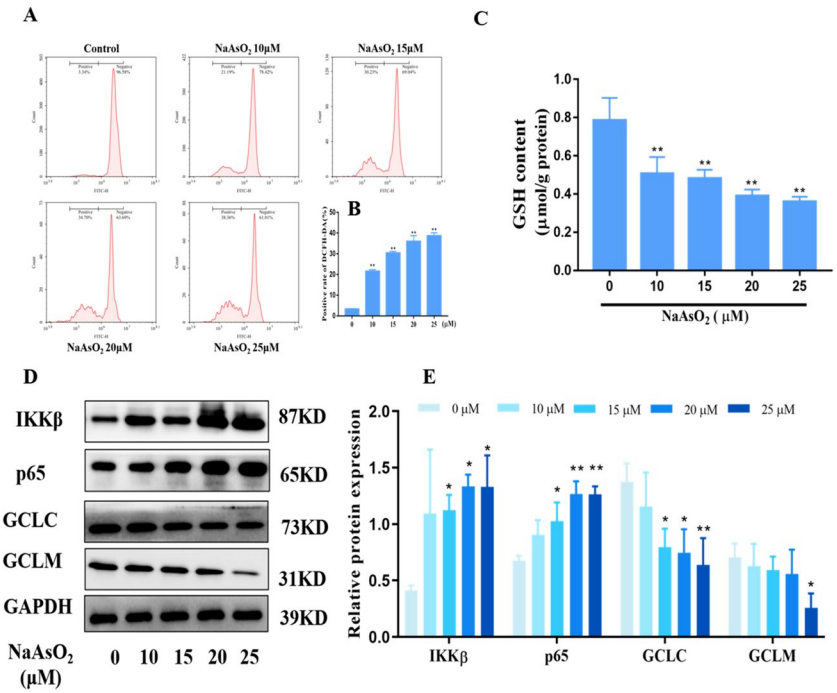

Fig. 4 $NaAsO_2$ induces oxidative stress through the NF-κB/GCLC signaling pathway. **A** Effect of different concentrations of $NaAsO_2$ on cellular ROS. **B** Quantitative data on the level of ROS treated with different concentrations of $NaAsO_2$. **C** Effect of different concentrations of $NaAsO_2$ on intracellular GSH. **D**, **E** The changes of IKKβ, p65, GCLC, and GCLM were detected after the cells were intervened with different concentrations of $NaAsO_2$ for 24 h. *Compared with the control group, $P < 0.05$. **Compared with the control group, $P < 0.01$, $n = 3$

breaks in the external mitochondrial membrane after the intervention with 15 μM and 25 μM $NaAsO_2$. The internal membrane and the ridge connection were also disrupted, and the ridge became blurred and invisible (Fig. 3A). The mitochondrial membrane potential of cells was significantly reduced after $NaAsO_2$ treatment (Fig. 3B,C).

After treating LX-2 cells with $NaAsO_2$, the levels of ROS were significantly increased compared with the control group (all $P<0.01$) (Fig. 4A,B). Meanwhile, we also detected the intracellular GSH content and found it significantly reduced exposure to $NaAsO_2$ (all $P<0.01$) (Fig. 4C). $NaAsO_2$ exposure significantly increased the protein expression of IKKβ and p65 and decreased the protein expression of GCLC and GCLM (all $P<0.05$). These results indicated that $NaAsO_2$ activated the NF-κB/GCLC pathway to induce apoptosis (Fig. 4D–E).

miR-214-5p Plays a Role in the Apoptosis of LX-2 Cells Induced by $NaAsO_2$

$NaAsO_2$ exposure significantly reduces the level of intracellular miR-214-5p (all $P<0.05$) (Fig. 5A). MiR-214-5p was highly expressed using miR-214-5p mimic, and mimic NC was used as a negative control and then combined with 15 μM $NaAsO_2$ for 24 h. Compared to the arsenic exposure group, the cell viability (Fig. 5B) and the GSH content (Fig. 5I) were significantly reduced. The apoptosis rate (Fig. 5C,D), the permeability of the mitochondrial membrane (Fig. 5E–F) and the level of ROS (Fig. 5G–H) were significantly increased (all $P<0.05$). Moreover, the protein expression of IKKβ and p65 was higher, and the expression level of GCLC protein was lower when the level of miR-214-5p was overexpressed (Fig. 5J,K).

LINC00942 Regulates the Expression of miR-214-5p Under the Effect of $NaAsO_2$

The dual luciferase reporter assay found that there was no significant difference in luciferase activity after mutating the binding sites of LINC00942 and miR-214-5p, indicating that LINC00942 can directly bind to miR-214-5p (Fig. 6A).

The results of FISH staining showed that after $NaAsO_2$ treatment, the green fluorescence intensity of LINC00942 increased, while the red fluorescence intensity of miR-214-5p decreased. More importantly, LINC00942 and miR-214-5p were distributed in the same position in the cells (Fig. 6B).

LINC00942 Plays a Role in the Apoptosis of LX-2 Cells Induced by $NaAsO_2$

When the concentration of $NaAsO_2$ reaches 15 μM at different times, the expression levels of LINC00942 were significantly increased (all $P<0.05$) (Fig. 7A). In the follow-up experiment of this study, the dose of $NaAsO_2$ was 15 μM, and the exposure time was 24 h. To further investigate the role of LINC00942 in $NaAsO_2$-induced apoptosis, we transfected si LINC00942 into cells, constructed a cell model with low expression of LINC00942, and transfected si NC into cells as a negative control, then combined with 15 μM $NaAsO_2$ for 24 h. It was found that the viability and GSH content (Fig. 7B,I) were significantly reduced. On the opposite, the apoptosis rate (Fig. 7C,D), mitochondrial membrane permeability (Fig. 7E,F), and the level of ROS were significantly increased (Fig. 7G,H) (all $P<0.05$). Moreover, the protein expression of IKKβ and p65

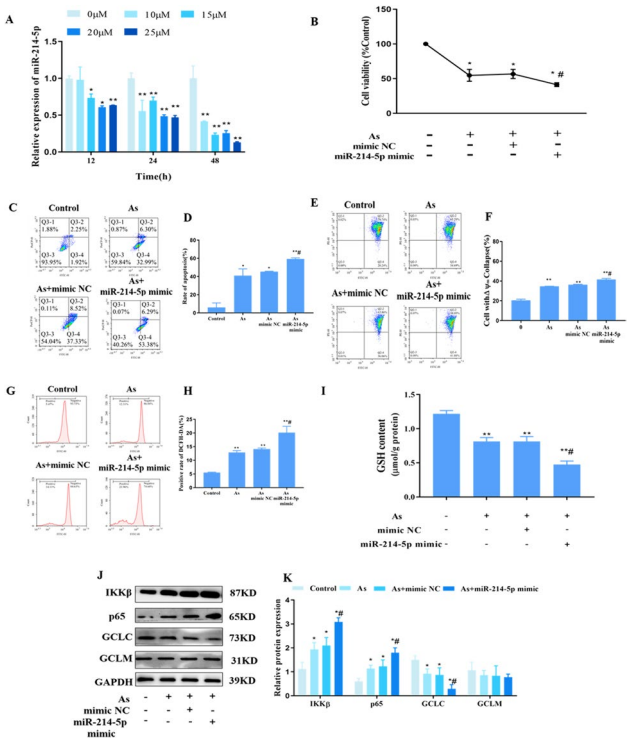

Fig. 5 Effects of miR-214-5p on $NaAsO_2$ inducing NF-κB, inhibiting GSH synthesis, and inducing cellular oxidative damage and apoptosis. **A** The expression level of miR-214-5p in LX-2 cells exposed to $NaAsO_2$ at different concentrations and at different times. **B** The effect of $NaAsO_2$ on cell viability after high expression of miR-214-5p. **C**, **D** The effect of $NaAsO_2$ on apoptosis rate after overexpression of miR-214-5p. **E**, **F** Effect of $NaAsO_2$ on mitochondrial membrane potential after high expression of miR-214-5p. **G**, **H** Effect of $NaAsO_2$ on ROS after high expression of miR-214-5p. **I** Effect of $NaAsO_2$ on GSH after high expression of miR-214-5p. **J**, **K** The effect of $NaAsO_2$ on IKKβ, p65, GCLC, and GCLM proteins after high expression of miR-214-5p. **B**–**K** The treatment concentration of $NaAsO_2$ was 15 μM, and the treatment time was 24 h. *Compared with the control group, $P<0.05$. **Compared with the control group, $P<0.01$. #Compared with the $NaAsO_2$ and mimic NC co-acting group, $n=3$

were higher, and the expression level of GCLC protein was lower in the $NaAsO_2$ plus si LINC00942 group (Fig. 7J,K).

LINC00942/miR-214-5p Regulates the Role of NF-κB/GCLC in $NaAsO_2$-induced Apoptosis

In order to further explore the role of LINC00942 in $NaAsO_2$-induced apoptosis through miR-214-5p, we constructed a cell model with low expression of LINC00942 and low expression of miR-214-5p. We found that in the case of $NaAsO_2$ exposure, reducing the expression of LINC00942 can restore the expression level of miR-214-5p. Then, the expression of miR-214-5p was inhibited after after adding miR-214-5p inhibitor (Fig. 8A).

In the presence of $NaAsO_2$, inhibition of the expression of LINC00942 significantly reduced cell viability; after inhibition of miR-214-5p expression, cell viability was restored (Fig. 8B). In contrast, the apoptosis rate of cells was significantly increased after the expression of LINC00942 was inhibited and decreased with the down-regulation of the expression level of miR-214-5p (Fig. 8C,D). The pro-apoptotic protein caspase 3, cleaved-caspase 3, and BAX/Bcl-2 ratio were significantly increased after LINC00942 reduction and were decreased after miR-214-5p expression was suppressed (all $P < 0.05$); the expression of anti-apoptotic protein Bcl-2 was decreased after the decrease of LINC00942 ($P < 0.05$) and increased after miR-214-5p decreased, but the difference was not statistically significant (Fig. 8E–J).

Inhibition of LINC00942 resulted in a decrease in intracellular mitochondrial membrane potential and GSH content and an increase in ROS levels. After jointly inhibiting the expression of miR-214-5p, compared with inhibiting LINC00942 alone, the mitochondrial membrane potential and GSH content of cells increased, while ROS levels decreased (Fig. 9A–E) (all $P < 0.05$). Treatment with si LINC00942 increased the expression levels of IKKβ and p65 and decreased the expression of GCLC. After combining with miR-214-5p inhibitor to inhibit the level of miR-214-5p, the protein expression levels of KKβ and p65 were reduced, and the expression of GCLC was increased (all $P < 0.05$). The expression changes of LINC00942 and miR-214-5p did not affect the levels of GCLC (Fig. 9F–J).

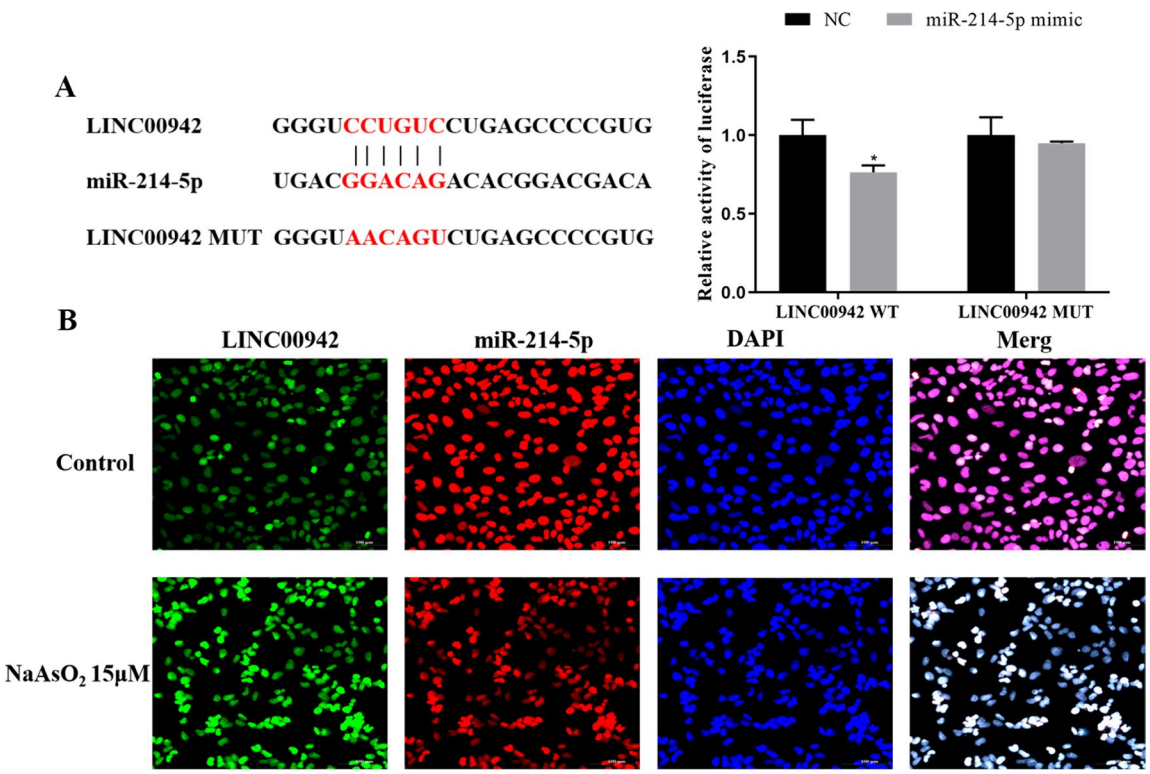

Fig. 6 Regulation of LINC00942 and miR-214-5p under the effect of $NaAsO_2$. **A** Binding sites of LINC00942 and miR-214-5p and dual luciferase report results. **B** Use FISH to locate the positions of LINC00942 and miR-214-5p in the cells, LINC00942 is stained with green light, and miR-214-5p is stained with dyed red. The treatment concentration of $NaAsO_2$ was 15 μM, and the treatment time was 24 h. *It indicates $P < 0.05$ compared with the control group, $n = 3$

Discussion

The hepatotoxicity induced by arsenic has become a research hotspot recently. In this study, we found that LINC00942 was induced to be highly expressed by $NaAsO_2$, which targeted and inhibited the expression of miR-214-5p. Reduction of miR-214-5p expression partially attenuated $NaAsO_2$ induced activation of NF-κB pathway and oxidative damage, which helps refine the theory of arsenic liver toxicity.

Several studies have shown that $NaAsO_2$ can increase the level of ROS, which in turn causes redox imbalance within the cells and ultimately induces apoptosis [20, 21]. GSH is a key antioxidant substance in cells, and the reduction of its synthesis is an important reason for redox imbalance. The synthesis of GSH is affected by the activity of the γ-glutamylcysteine synthetase (γ-GCS). γ-GCS is composed of two subunits, GCLC and GCLM, of which GCLC plays a major role in the generation of GSH [22]. A previous study found that GCLC protein and mRNA were negatively regulated by NF-κB under the effect of $NaAsO_2$, further affecting the production of GSH. Finally, it increased the level of apoptosis [3]. These conclusions are consistent with our results.

LINC00942 is a proto-oncogene, and its aberrant expression is associated with a variety of malignant tumors [23–25]. In this experiment, we found that LINC00942 is elevated with arsenic exposure and plays a compensatory role in the process of fighting oxidative stress. It has been found that the overproduction of ROS in hepatocytes under the action of arsenic

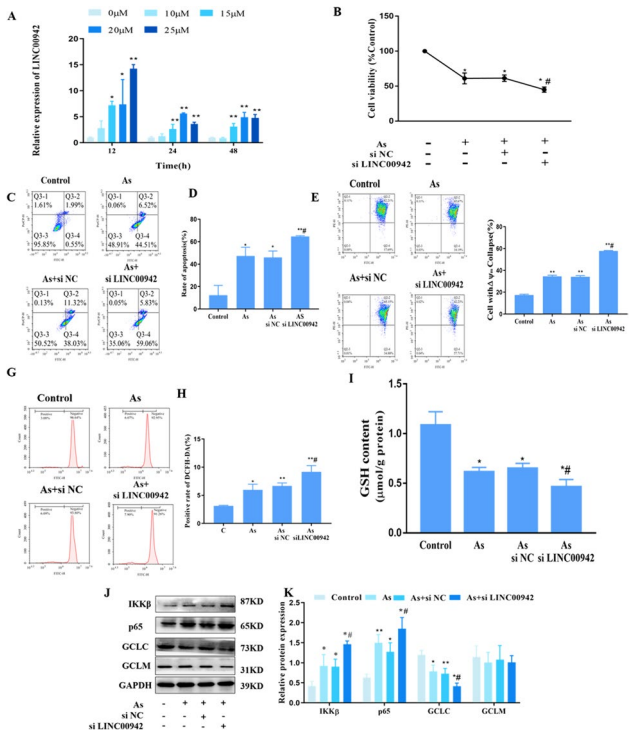

Fig. 7 Effects of LINC00942 on $NaAsO_2$ inducing NF-κB, inhibiting GSH synthesis, and inducing cellular oxidative damage and apoptosis. **A** The expression level of LINC00942 in LX-2 cells exposed to arsenic at different concentrations and at different times. **B** The effect of $NaAsO_2$ on cell viability after inhibiting the expression level of LINC00942. **C**, **D** The effect of $NaAsO_2$ on the apoptosis rate after inhibiting the expression level of LINC00942. **E**, **F** Effect of $NaAsO_2$ on mitochondrial membrane potential after inhibiting LINC00942 expression level. **G**, **H** The effect of $NaAsO_2$ on ROS after LINC00942 expression level. **I** The effect of $NaAsO_2$ on GSH after inhibiting the expression level of LINC00942. **J**, **K** The effect of $NaAsO_2$ on IKKβ, p65, GCLC, and GCLM proteins after inhibiting the expression level of LINC00942. **B–K** The treatment concentration of $NaAsO_2$ was 15 μM, and the treatment time was 24 h.*Compared with the control group, $P<0.05$. **Compared with the control group, $P<0.01$. #Compared with arsenic and si NC co-acting group, $P<0.05$, $n=3$

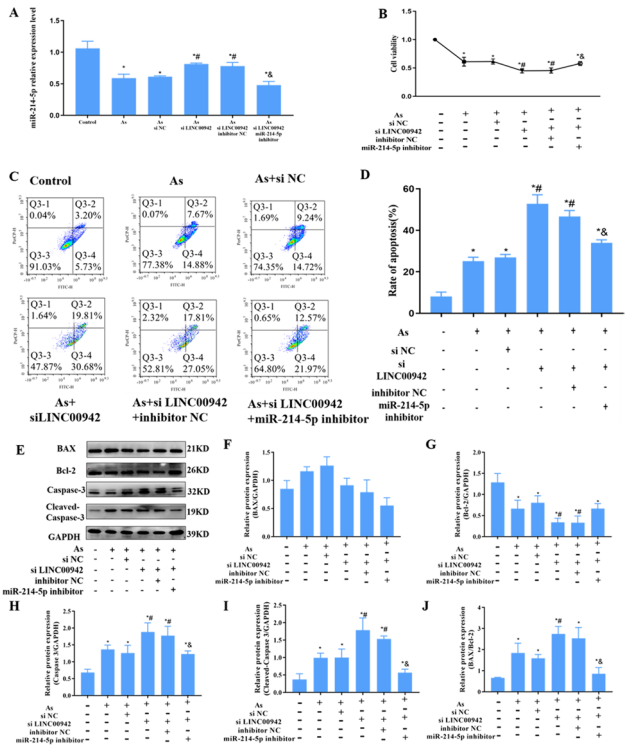

Fig. 8 LINC00942 regulates $NaAsO_2$-induced apoptosis by miR-214-5p. **A** The expression level of miR-214-5p in cells after different treatments. **B** The viability of cells after different treatments. **C**, **D** The apoptosis level of LX-2 cells detected by flow cytometry Q3-1 indicates mechanically injured cells; Q3-2 indicates late apoptotic cells; Q3-3 indicates normal cells; Q3-4 indicates early apoptotic cells. **E–J** Western blotting images and quantitative data of relative expression level of BAX, Bcl-2, caspase 3, cleaved-caspase 3, Bax/Bcl-2 indicates comparison with the control group, $P<0.05$. #It indicates comparison with the As + si NC group, $P<0.05$. &It indicates comparison with the As + si LINC00942 + NC inhibitor group, $P<0.05$, $n=3$

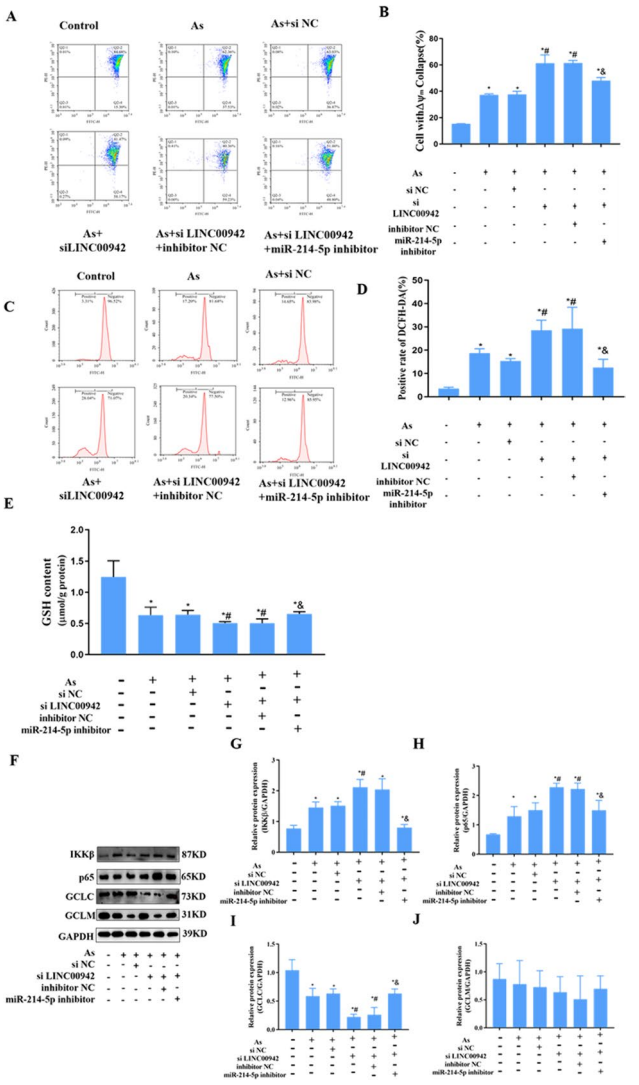

Fig. 9 LINC00942 regulates the effects of miR-214-5p on cellular oxidative stress and the NF-κB/GCLC pathway in $NaAsO_2$. **A**, **B** The effect of different treatments on mitochondrial membrane potential. **C**, **D** The effect of different treatments on cellular ROS. **E** The effect of different treatments on intracellular GSH. **F–J** The effect of $NaAsO_2$ on IKKβ, p65, GCLC, and GCLM proteins. *It indicates a comparison with the control group, $P<0.05$. #It indicates comparison with the As + si NC group, $P<0.05$. &It indicates comparison with the As + si LINC00942 + NC inhibitor group, $P<0.05$, $n=3$

leads to the compensatory reaction of cells to enhance the antioxidant capacity of cells [26]. LINC00942 is positively regulated by the cellular antioxidant protein Nrf2 [19]. Several studies have shown that arsenic exposure can induce the production of reactive oxygen species and increase the expression of Nrf2 [27–29]. These results suggest that arsenic-induced oxidative stress can activate the Nrf2 signaling pathway through cellular compensatory action, thereby increasing the level of LINC00942 and playing a role in resisting oxidative damage.

Dual luciferase reporter assays determined that LINC00942 can target to reduce miR-214-5p expression directly. In the cytoplasm, the precursor miR-214 is recognized and processed by Dicer to produce mature miR-214-5p, which has a role in regulating NF-κB [10] and inducing oxidative damage [30, 31]. Our experiments showed that miR-214-5p was lowly expressed after $NaAsO_2$ treatment. After transfection of the plasmid to make miR-214-5p highly expressed, the NF-κB signaling pathway protein p65 was highly expressed, and oxidative damage was more severe compared to the arsenic group. Xu [10] et al. found that miR-214-5p could target PPARGC1B to promote the expression level of NF-κB pathway-related proteins inducing chondrocyte inflammation and apoptosis. In addition, Gao et al. [8] experimentally demonstrated that under arsenic trioxide exposure, high expression of Nrf2 targeted and inhibited miR-214-5p, which elevated the expression of ATF4 and EZH2 and suppressed the apoptosis rate of cells.

In addition, we also found that the protein expression of GCLC of the treatment group of arsenic and si LINC00942 was lower compared with that of the arsenic-exposed group, and the level of intracellular ROS and the apoptosis rate were increased. ASHOURI et al. [32] found that ASOs (antisense oligonucleotides) of LINC00942 can reduce the mRNA expression of GCLC in A549 cells. It is shown that the mRNA expression of GCLC was reduced after inhibiting LINC00942. Under the combined effect of $NaAsO_2$ and si LINC00942, compared with the $NaAsO_2$ group, miR-214-5p was restored, the expression of p65 increased, and the protein content of GCLC decreased. These results could be attributed to the fact that high expression of miR-214-5p due to the inhibition of LINC00942, which induced the expression of PPARGC1B decreased, and then p65, as the downstream of PPARGC1B, was upregulated, while the GCLC protein was downregulated.

The present study investigated the role of LINC00942 in $NaAsO_2$-induced LX-2 cells by targeting miR-214-5p to regulate the NF-κB pathway, but there are still shortcomings. The long-term effect of $NaAsO_2$ on LINC00942 is still unclear and requires further experimental exploration. The specific mechanism between miR-214-5p and NF-κB was not explored in depth; moreover, this experiment was conducted in vitro only in LX-2 cells, which could not directly prove the damaging effect of $NaAsO_2$ on human liver tissue, and further experiments are needed to verify the harmful effect of liver induced by arsenic (Fig. 10).

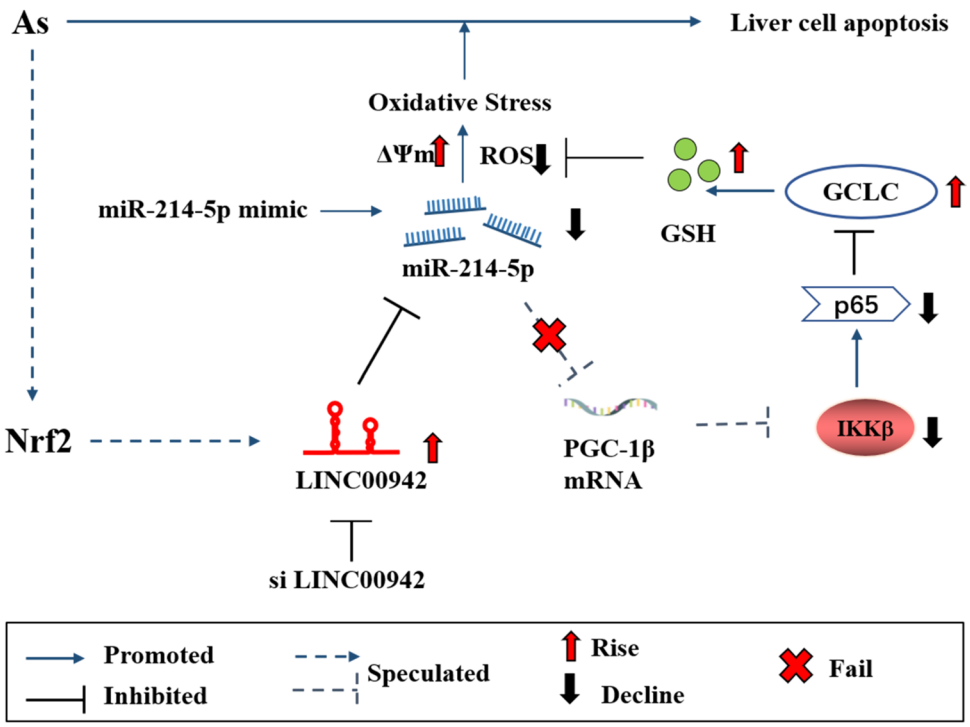

Fig. 10 The role of LINC00942/miR-214-5p in $NaAsO_2$ regulation of NF-κB/GCLC pathway expression and induction of cell apoptosis. $NaAsO_2$ exposure induces oxidative damage and apoptosis in LX-2 cells by activating NF-κB and inhibiting GSH synthesis. During this process, the expression level of LINC00942 increases, targeting to reduce the level of miR-214-5p, then weakening the effect of $NaAsO_2$ on NF-κB, thereby alleviating cellular oxidative damage and playing a potential protective role. After inhibiting the expression of LINC00942, $NaAsO_2$ exposure increased the expression of miR-214-5p, further activated NF-κB to inhibit the synthesis of GSH, and then induced oxidative damage

Conclusion

$NaAsO_2$ exposure induces oxidative damage and apoptosis in LX-2 cells by activating NF-κB and inhibiting GSH synthesis. During this process, the expression level of LINC00942 increases, targeting to reduce the level of miR-214-5p, then weakening the effect of $NaAsO_2$ on NF-κB, thereby alleviating cellular oxidative damage and playing a protective role.

Author Contributions All authors contributed to the study conception and design. Material preparation, data collection were performed by Mingxiao Ma and Jingyi Zhang. Formal analysis and Visualization were performed by Sheng Li, Mengyao Zhang, Weixin Chen and Linzhi Li. The frst draft of the manuscript was written by Mingxiao Ma and Jingyi Zhang.Conceptualization, Methodology, Supervision and Writing—review and editing were performed by Shugang Li. All authors approved the final manuscript.

Funding This work was supported by grants from the Capital Medical University Cultivation Fund Project PYZ21017.

Data Availability No datasets were generated or analyzed during the current study.

Declarations

Competing Interests The authors declare no competing interests.

References

1. Chen QY, Costa M (2021) Arsenic: a global environmental challenge. Annu Rev Pharmacol Toxicol 61(1):47–63. https://doi.org/10.1146/annurev-pharmtox-030220-013418
2. Jahangirnejad R, Goudarzi M, Kalantari H et al (2020) Subcellular organelle toxicity caused by arsenic nanoparticles in isolated rat hepatocytes. Int J Occup Environ Med 11(1):41–52. https://doi.org/10.15171/ijoem.2020.1614
3. Ran S, Gao X, Ma M et al (2022) $NaAsO_2$ decreases GSH synthesis by inhibiting GCLC and induces apoptosis through Hela cell mitochondrial damage, mediating the activation of the NF-kappaB/miR-21 signaling pathway. Ecotoxicol Environ Saf 234:113380. https://doi.org/10.1016/j.ecoenv.2022.113380
4. Hou J, Zhang J, Cui P et al (2021) TREM2 sustains macrophage-hepatocyte metabolic coordination in nonalcoholic fatty liver disease and sepsis. J Clin Invest 131(4):e135197. https://doi.org/10.1172/jci135197
5. Wei CX, Yan A, Xu T et al (2020) miRNA-150-5p promotes hepatic stellate cell proliferation and sensitizes hepatocyte apoptosis during liver fibrosis. Epigenomics 12(1):53–67. https://doi.org/10.2217/epi-2019-0104
6. Xu Y, Zhu Y, Hu S et al (2021) Hepatocyte miR-34a is a key regulator in the development and progression of non-alcoholic fatty liver disease. Mol Metab 51:101244. https://doi.org/10.1016/j.molmet.2021.101244
7. Li L, Ai R, Yuan X et al (2023) LINC00886 facilitates hepatocellular carcinoma tumorigenesis by sequestering microRNA-409-3p and microRNA-214-5p. J Hepatocell Carcinoma 10:863–881. https://doi.org/10.2147/jhc.s410891
8. Gao M, Liu Y, Chen Y et al (2016) miR-214 protects erythroid cells against oxidative stress by targeting ATF4 and EZH2. Radic Biol Med 92:39–49. https://doi.org/10.2147/jhc.s410891

9. Zhou ZQ, Qi M, Cao Q et al (2021) Effects of metoprolol on oxidative stress injury of hypoxia and high glucose cardiomyocytes by targeting miR-214–5p through ZFAS. J Toxicol 35(04):297–304. https://doi.org/10.16421/j.cnki.1002-3127.2021.04.007
10. Xu J, Pei Y, Lu J et al (2020) LncRNA SNHG7 alleviates IL-1beta-induced osteoarthritis by inhibiting miR-214-5p-mediated PPARGC1B signaling pathways. Int Immunopharmacol 90:107150. https://doi.org/10.1016/j.intimp.2020.107150
11. Chen Y, Li S, Zhang Y et al (2021) The lncRNA Malat1 regulates microvascular function after myocardial infarction in mice via miR-26b-5p/Mfn1 axis-mediated mitochondrial dynamics. Redox Biol 41(10):101910. https://doi.org/10.1016/j.redox.2021.101910
12. Cheng T, Xu M, Qin B et al (2019) lncRNA H19 contributes to oxidative damage repair in the early age-related cataract by regulating miR-29a/TDG axis. J Cell Mol Med 23(9):6131–6139. https://doi.org/10.1111/jcmm.14489
13. Wei C, Sun Y, Wang J et al (2021) LncRNA NONMMUT055714 acts as the sponge of microRNA-7684–5p to protect against postoperative cognitive dysfunction. Aging 3(9):12552–12564 (10.18632/aging.202932)
14. Teng Y, Ding M, Wang X et al (2020) LncRNA RMRP accelerates hypoxia-induced injury by targeting miR-214-5p in H9c2 cells. J Pharmacol Sci 142(2):69–78. https://doi.org/10.1016/j.jphs.2019.07.014
15. Chen X, Sun C, Liu C et al (2021) Research progress of LncRNA and hepatic glucose and lipid metabolism. Chin J Bioeng 37(1):40–52. https://doi.org/10.3389/fphar.2023.1256705
16. Yan Q, Hu Q, Li G (2023) NEAT1 regulates calcium oxalate crystal-induced renal tubular oxidative injury via miR-130/IRF1. Antioxid Redox Signal 38(10–12):731–746. https://doi.org/10.1089/ars.2022.0008
17. Sun T, Wu Z, Wang X et al (2020) LNC942 promoting METTL14-mediated m(6)A methylation in breast cancer cell proliferation and progression. Oncogene 39(31):5358–5372. https://doi.org/10.1038/s41388-020-1338-9
18. Hu H, Xu H, Lu F et al (2020) Exploring the effect of differentially expressed long non-coding RNAs driven by copy number variation on competing endogenous RNA network by mining lung adenocarcinoma data. Front Cell Dev Biol 8:627436. https://doi.org/10.3389/fcell.2020.627436
19. Richter K, Konzack A, Pihlajaniemi T et al (2015) Redox-fibrosis: impact of TGFbeta1 on ROS generators, mediators and functional consequences. Redox Biol 6:344–352. https://doi.org/10.1016/j.redox.2015.08.015
20. Liu C, Zhang A (2020) ROS-mediated PERK-eIF2alpha-ATF4 pathway plays an important role in arsenite-induced L-02 cells apoptosis via regulating CHOP-DR5 signaling. Environ Toxicol 35(10):1100–1113. https://doi.org/10.1002/tox.22946
21. Hu Y, Li J, Lou B et al (2020) The role of reactive oxygen species in arsenic toxicity. Biomolecules 10(2):240. https://doi.org/10.3390/biom10020240
22. Chen Y, Dong H, Thompson DC et al (2013) Glutathione defense mechanism in liver injury: insights from animal models. Food Chem Toxicol 60:38–44. https://doi.org/10.1016/j.fct.2013.07.008
23. Zhu Y, Zhou B, Hu X et al (2022) LncRNA LINC00942 promotes chemoresistance in gastric cancer by suppressing MSI2 degradation to enhance c-Myc mRNA stability. Clin Transl Med 12(1):e703. https://doi.org/10.1002/ctm2.703
24. Xu Z, Peng B, Liang Q et al (2021) Construction of a ferroptosis-related nine-lncRNA signature for predicting prognosis and immune response in hepatocellular carcinoma. Front Immunol 12–719175. https://doi.org/10.3389/fimmu.2021.719175
25. Zhang L, Li L, Zhan Y et al (2020) Identification of immune-related lncRNA signature to predict prognosis and immunotherapeutic efficiency in bladder cancer. Front Oncol 10–542140. https://doi.org/10.3389/fonc.2020.542140
26. Rezaei M, Keshtzar E, Khodayar MJ et al (2019) SirT3 regulates diabetogenic effects caused by arsenic: an implication for mitochondrial complex II modification. Toxicol Lett 301:24–33. https://doi.org/10.1016/j.toxlet.2018.10.025
27. Sun HJ, Ding S, Guan DX et al (2022) Nrf2/Keap1 pathway in countering arsenic-induced oxidative stress in mice after chronic exposure at environmentally-relevant concentrations. Chemosphere 303(Pt 3):135256. https://doi.org/10.1016/j.chemosphere.2022.135256
28. Liu P, Dodson M, Li H et al (2021) Non-canonical NRF2 activation promotes a pro-diabetic shift in hepatic glucose metabolism. Mol Metab 51–101243. https://doi.org/10.1016/j.molmet.2021.101243
29. Silva-adaya D, Ramos-chavez LA, Petrosyan P et al (2020) Early neurotoxic effects of inorganic arsenic modulate cortical GSH levels associated with the activation of the Nrf2 and NFkappaB pathways, expression of amino acid transporters and NMDA receptors and the production of hydrogen sulfide. Front Cell Neurosci 25(14):17. https://doi.org/10.3389/fncel.2020.00017
30. Guo C, Ye FX, Jian YH et al (2022) MicroRNA-214-5p aggravates sepsis-related acute kidney injury in mice. Drug Dev Res 83(2):339–350. https://doi.org/10.1002/ddr.21863
31. Wang P, Li ZW, Zhu Z et al (2019) Inhibition of miR-214–5p attenuates inflammatory chemotaxis and nerve regeneration obstruction after spinal cord injury in rats. Eur Rev Med Pharmacol Sci 23(6):2332–9. https://doi.org/10.26355/eurrev_201903_17376
32. Ashouri A, Sayin VI, Van Den Eynden J et al (2016) Pan-cancer transcriptomic analysis associates long non-coding RNAs with key mutational driver events. Nat Commun 7:13197. https://doi.org/10.1038/ncomms13197